Video Article

# Slice Patch Clamp Technique for Analyzing Learning-Induced Plasticity

Hiroyuki Kida[1], Yuya Sakimoto[1], Dai Mitsushima[1]

[1]Department of Physiology, Yamaguchi University Graduate School of Medicine

Correspondence to: Dai Mitsushima at mitsu@yamaguchi-u.ac.jp

URL: https://www.jove.com/video/55876
DOI: doi:10.3791/55876

Keywords: Neuroscience, Issue 129, Patch clamp, primary motor cortex, hippocampus, motor learning, contextual learning, AMPA receptor, glutamate, $GABA_A$ receptor, GABA, synaptic plasticity, rat

Date Published: 11/11/2017

Citation: Kida, H., Sakimoto, Y., Mitsushima, D. Slice Patch Clamp Technique for Analyzing Learning-Induced Plasticity. *J. Vis. Exp.* (129), e55876, doi:10.3791/55876 (2017).

## Abstract

The slice patch clamp technique is a powerful tool for investigating learning-induced neural plasticity in specific brain regions. To analyze motor-learning induced plasticity, we trained rats using an accelerated rotor rod task. Rats performed the task 10 times at 30-s intervals for 1 or 2 days. Performance was significantly improved on the training days compared to the first trial. We then prepared acute brain slices of the primary motor cortex (M1) in untrained and trained rats. Current-clamp analysis showed dynamic changes in resting membrane potential, spike threshold, afterhyperpolarization, and membrane resistance in layer II/III pyramidal neurons. Current injection induced many more spikes in 2-day trained rats than in untrained controls.

To analyze contextual-learning induced plasticity, we trained rats using an inhibitory avoidance (IA) task. After experiencing foot-shock in the dark side of a box, the rats learned to avoid it, staying in the lighted side. We prepared acute hippocampal slices from untrained, IA-trained, unpaired, and walk-through rats. Voltage-clamp analysis was used to sequentially record miniature excitatory and inhibitory postsynaptic currents (mEPSCs and mIPSCs) from the same CA1 neuron. We found different mean mEPSC and mIPSC amplitudes in each CA1 neuron, suggesting that each neuron had different postsynaptic strengths at its excitatory and inhibitory synapses. Moreover, compared with untrained controls, IA-trained rats had higher mEPSC and mIPSC amplitudes, with broad diversity. These results suggested that contextual learning creates postsynaptic diversity in both excitatory and inhibitory synapses at each CA1 neuron.

AMPA or $GABA_A$ receptors seemed to mediate the postsynaptic currents, since bath treatment with CNQX or bicuculline blocked the mEPSC or mIPSC events, respectively. This technique can be used to study different types of learning in other regions, such as the sensory cortex and amygdala.

## Video Link

The video component of this article can be found at https://www.jove.com/video/55876/

## Introduction

The patch clamp technique, developed by Neher and Sakmann, has been widely used for electrophysiological experiments[1]. The whole-cell patch clamp technique[2] can be used to record intracellular current or voltage using the gigaohm seal of the cell membrane. The current-clamp technique allows us to analyze differences in membrane properties such as resting potential, resistance, and capacitance[3]. The voltage-clamp technique allows us to analyze learning-induced synaptic plasticity at both excitatory and inhibitory synapses.

The primary motor cortex (M1) is a central region that is critical for making skilled voluntary movements. Previous electrophysiological studies demonstrated the development of long-term potentiation (LTP)-like plasticity in layer II/III excitatory synapses after skilled motor training[4]. Moreover, *in vivo* imaging studies further demonstrated the remodeling of M1 dendritic spines after a skilled reaching task[5,6]. However, learning-induced synaptic and intrinsic plasticity has not been shown in M1 neurons.

We recently reported that a rotor rod task promoted dynamic changes in glutamatergic and GABAergic synapses and altered the intrinsic plasticity in M1 layer II/III neurons[7]. Here we used the slice patch clamp technique to investigate learning-induced plasticity. This technique can also be used to investigate other types of experience-dependent plasticity in other brain regions. For example, sensory input into the barrel cortex can strengthen AMPA receptor-mediated excitatory input into layer II/III neurons[8], and cued fear conditioning strengthens the excitatory inputs onto the lateral amygdala neurons, which is required for fear memory[9]. Moreover, contextual learning creates diversity in terms of excitatory and inhibitory synaptic input into hippocampal CA1 neurons[10,11].

## Protocol

All animal housing and surgical procedures were in accordance with the Guidelines for Animal Experimentation of Yamaguchi University School of Medicine and were approved by the Institutional Animal Care and Use Committee of Yamaguchi University.

## 1. Animals

1. Use 4- to 5-week-old male Sprague-Dawley rats (postnatal 28 to 31 days of age).
2. House the rats in individual plastic cages (40 cm × 25 cm × 25 cm) maintained at a constant temperature (23 °C ± 1 °C) under a 12-h light/dark cycle. Give rats *ad libitum* access to water and food.

## 2. Rotor rod test

1. To investigate motor skill learning, *subject each rat* to the rotor rod test (rod diameter 7 cm; lane width 8.9 cm; fall height 26.7 cm) for 1 or 2 consecutive days (**Figure 1A** in Kida et al., 2016[7]). Perform the task in a quiet, temperature-controlled room (23 ± 1 °C). Do not disturb or handle rats prior to the test.
2. Set the rotor rod to acceleration mode, which increases linearly from 4 rotations/min to 40 rotations/min (8 π/min to 80 π/min) in 5 min.
3. Put the rat on the resting rotating rod. Confirm that all limbs are on the rod.
4. Measure the latency to fall from the rotating rod to evaluate motor performance.
5. Allow each rat 10 attempts (trials) with 30-s intervals.
6. If the rat falls from the rotating rod, set it on the rod again after a 10-20 s interval.
7. Sacrifice the rat with an overdose of pentobarbital (400 mg/kg) 30 min after the final trial. Inject untrained control rats with the same dose of anesthesia in their home cages.

## 3. Inhibitory avoidance test

1. To investigate contextual learning, subject rats to an inhibitory avoidance (IA) test (**Figure 1D** in Mitsushima et al., 2011, 2013[10,11]) Avoid any episodic experiences on the day of the experiment such as contact with others, cage changes or cleaning. Perform the task in a quiet, temperature-controlled room (23 ± 1 °C).
   NOTE: The IA training apparatus is a two-chambered acrylic box (length 33 cm; width 58 cm; height 33 cm). It has a lighted safe side and a dark shock side that are separated by a trap door (**Figure 1D**).
2. Place the rat in the safe (lit) side of the illuminated box. Handle the rat gently without stress.
3. Wait a short time (10 to 20 s) to acclimate the rat to the environment.
4. Open the sliding door to allow the rat to enter the dark box at will.
5. Measure the latency (s) before the rat enters the novel dark side of the box. The latency of the first trial represents the rat's performance before training.
6. After entry into the dark side, close the door and apply a scrambled electrical foot shock (2 s, 1.6 mA) via electrical steel rods set into the floor of the box. Allow walk-through rats to explore the training apparatus for 1 min without being shocked. House unpaired rats in an illuminated shock cage for several days and suddenly give the shock without episodic experiences. Handle gently without stress in any groups.
7. Keep each rat in the dark box for 10 s before returning it to the home cage.
8. At 30 min after the foot shock, again place the rat into the lighted side of the box. Measure the latency to enter the dark side.
9. Return the rat to the home cage.
10. At 60 min after the shock, sacrifice the rat with an overdose of pentobarbital (400 mg/kg). Handle the rat gently and inject the anesthesia intraperitoneally. In untrained control rats, inject the anesthesia in their home cages without the experience described above.

## 4. Dissection buffer

1. Dissolve crystals of 0.195 g $NaH_2PO_4$-$2H_2O$, 0.188 g KCl, 0.074 g $CaCl_2$, 1.423 g $MgCl_2$-$6H_2O$, and 12.579 g choline chloride in ultrapure water (900 mL to 950 mL). See Table 1.
2. Dissolve crystals of 2.340 g ascorbic acid, 0.342 g pyruvic acid sodium salt, 2.100 g $NaHCO_3$, and 4.500 g glucose.
3. Add water up to 1000 mL. The range of osmolality will be between 290 mOsm/L and 300 mOsm/L. Adjust osmolality by adding ultrapure water, if it is over the range.
4. Bubble the solution with 5% $CO_2$/95% $O_2$ gas mixture at ice-cold temperatures for 5 min before use.

## 5. Artificial cerebrospinal fluid (aCSF)

1. Dissolve crystals of 0.186 g KCl, 6.700 g NaCl, and 0.156 g $NaH_2PO_4$-$2H_2O$ in ultrapure water (900 mL to 950 mL). See Table 2.
2. Bubble with the gas mixture for 5 min.
3. Dissolve crystals of 1.800 g glucose and 2.184 g $NaHCO_3$ and then add 4 mL $MgCl_2$ and 4 mL $CaCl_2$ from 1 M stock solutions.
4. Add water up to 1000 mL. The range of osmolality will be between 290 mOsm/L and 295 mOsm/L. Adjust osmolality by adding ultrapure water, if it is over the range.
5. Bubble with the gas mixture prior to use.

## 6. Intracellular solutions

1. For current-clamp recordings (Table 3), dissolve 0.0746 g KCl, 6.089 g K-gluconate, 0.476 g HEPES, 0.0456 g EGTA, and 500 µL $MgCl_2$ from 1 M stock solution in 180 mL ultrapure water (adjust pH to 7.2 with KOH).
   1. Add 0.4408 g $Na_2$-ATP, 0.0418 g $Na_3$-GTP, and 0.510 g Na-phosphocreatine. Add water to 200 mL and adjust the pH to 7.35 with KOH.
   2. Adjust the osmolality to around 290 mOsm/L by adding ultrapure water.
   3. Store as 1-mL aliquots in the freezer (-30 °C).

2. For voltage-clamp recordings (Table 4), dissolve 5.244 g $CsMeSO_3$, 0.672 g CsCl, 0.476 g HEPES, 0.0456 g EGTA, and 500 µL $MgCl_2$ from 1 M stock solutions in 180 mL ultrapure water. Adjust the pH to 7.2 with CsOH. For mEPSP and mIPSP recordings, use modified concentration of 5.814 g $CsMeSO_3$ and 0.252 g CsCl to adjust the reversal potential of the $GABA_A$ receptor response[11].
    1. Add 0.4408 g $Na_2$-ATP, 0.0418 g $Na_3$-GTP, and 0.510 g Na-phosphocreatine. Add water to 200 mL and adjust the pH to 7.35 with CsOH.
    2. Adjust the osmolality to around 290 mOsm/L by adding ultrapure water .
    3. Store as 1-mL aliquots in the freezer (-30 °C).

## 7. Slice preparation

1. Prior to sacrifice, cool-down all dissection tools with crushed ice (**Figure 2A**). Add about 500 mL of cold water into the crushed ice container to increase the contact surface area. This procedure was described previously[10,11,12].
   NOTE: The tools here are: Large scissors, iris scissors, a spatula, a micro spatula, forceps, tweezers, a stainless steel 200-mL beaker, a blade for brain trimming, a 120-mL cardiac perfusion syringe filled with dissection buffer treated with the gas mixture, a silicone tube (20 cm) connected to a flattened 18-gauge needle, a stainless brain dissection stage (thickness = 3 mm, ϕ = 12 cm), and a mounting stage for the vibratome (ϕ = 5 cm).
2. Sacrifice the rat 30 min after completing the behavioral paradigm by anesthetizing it with an overdose of pentobarbital (400 mg/kg bodyweight). Perform the slice preparation rapidly to ensure that the slices are as healthy as possible[10,11,12]. The brain extraction protocol meets all veterinary standards for our university.
3. Fill a 120-mL syringe with ice-cold dissection buffer (Table 1) bubbled with a 5% $CO_2$/95% $O_2$ gas mixture. Remove any air bubbles prior to perfusion.
4. After exposing the heart, insert the needle into the posterior part of the left ventricle.
5. Perform transcardial perfusion of the brain manually using the syringe. Larger rats require more dissection buffer for perfusion. Submerge the brain with ice-cold dissection buffer for 5 min. Bubble the buffer continuously during the submersion.
6. Trim the posterior side of the brain at an angle parallel to the dendritic orientation of the target cortical region using a blade. Since the brain is stand on dissection stage with the cut end bottom, the initial angle determines the angle of all subsequent brain slices. This step is **critically important** (**Figure 2B**). An incorrect angle may cut through the target pyramidal neurons.
   NOTE: The tools here are: a blade for brain trimming, a filter paper (ϕ = 10 cm), a stainless brain dissection stage (thickness = 3 mm, ϕ = 12 cm), a spatula, a superglue, a dropper, and a mounting stage for the vibratome (ϕ = 5 cm).
7. Cut 350-µm thick coronal brain slices using a vibratome. Fill the dissection chamber with ice-cold buffer bubbled with a 5% $CO_2$/95% $O_2$ gas mixture (**Figure 2C**). Bubble the buffer continuously during the brain slice.
8. Trim the periphery of the target area using iris scissors.
9. Wash the trimmed slices gently in room temperature aCSF bubbled with 5% $CO_2$/95% $O_2$ (Table 2).
10. Maintain the trimmed slices in an interface chamber until the recording is performed (**Figure 2D** and **E**). Incubation for 1 h in the chamber improves the condition of the cells, but the phenotypes change if the slices are incubated for more than 10 hours. Close the lid of the chamber to enclose the gases and the small liquid drops of aCSF.

## 8. Whole-cell patch clamp

NOTE: Whole-cell recordings require an amplifier and a low-pass filter that is set to a cutoff frequency of 5 kHz. The signals are digitized and stored in a PC. The stored data are analyzed offline (**Figure 3A**).

1. Create glass electrodes using a horizontal puller. Fill the electrodes with a suitable solution (Tables 3 and 4) using a regular polyethylene 1-mL syringe attached to a fine glass tube and a 0.22-µm filter.
2. Prior to contact with the cell, maintain positive pressure and adjust the pipette current to zero.
3. After forming a gigaohm seal, apply negative pressure to rupture the cell membrane (whole-cell configuration in **Figure 3F**).

## 9. Current-clamp analysis

1. Properties of the cell membrane
    1. Fill the patch recording pipettes with the intracellular solution for current-clamp recordings (Table 3). The resistance of the pipette is between 4 MΩ and 7 MΩ in the aCSF.
    2. After the membrane ruptures, hold the membrane voltage at -60 mV in V-CLAMP mode. Then, switch from "bath" mode to "cell" mode in the membrane test using software to measure the intrinsic cell properties such as membrane capacitance, resistance, and time constant.

2. Current injection study
    1. After recording the intrinsic cell properties, switch the mode from V-CLAMP to TRACK (I = 0) /I-CLAMP NORMAL for the current injection. Note that the liquid junction potential should not be corrected[10].
    2. Inject current into the cell for 300 ms. Change the intensity of the current stepwise from −100 pA to +550 pA with 50-pA increases. Count the number of spikes (action potentials) elicited by the current injections.
    3. Measure the minimum voltage needed to induce an action potential (this is the threshold voltage).
    4. Calculate the afterhyperpolarization amplitude as the difference between the voltage at spike initiation and the lowest voltage attained during afterhyperpolarization[7].

## 10. Voltage-clamp analysis

1. The AMPA/NMDA ratio
   NOTE: The AMPA/NMDA ratio is a conventional way to evaluate postsynaptic plasticity at glutamatergic excitatory synapses[7,8,9,10,11]. However, note that concomitant increases in both components may not change the ratio[13].
   1. Perfuse the recording chamber with physiological solution bubbled with the gas mixture and maintain the temperature at 22 °C to 25 °C. Add 0.1 mM picrotoxin to the solution to block the $GABA_A$-mediated response and add 4 µM 2-chloroadenosine to stabilize the evoked neural response[14].
   2. Fill the patch recording pipettes with the intracellular solution for voltage-clamp recordings (Table 4). Check the resistance of the recording pipette in the aCSF. The resistance is between 4 MΩ and 7 MΩ.
   3. For recording in layer II/III pyramidal neurons in the M1, place a bipolar tungsten stimulating electrode 200 µm to 300 µm lateral to the cells to be recorded, below the pial surface in the region of the forelimb representation (2-mm lateral to the midline)[15,16,17].
   4. For recording in a CA1 pyramidal neuron, place the stimulating electrode 200 µm to 300 µm lateral (Schaffer collateral fiber) or medial (temporoammonic pathway) to the cells that will be recorded (**Figure 3B**).
   5. Increase the stimulus intensity up to the synaptic response > 10 pA.
   6. Calculate the AMPA/NMDA ratio as the ratio of the peak current measured at −60 mV to the current measured at +40 mV at 150 msec after the stimulus onset. Note that 50 to 100 traces should be averaged to calculate the ratio.

2. Miniature postsynaptic current recordings
   Note: Miniature excitatory postsynaptic currents (mEPSCs) are thought to correspond to the responses elicited by the presynaptic release of a single vesicle of glutamate[18]. In contrast, miniature inhibitory postsynaptic currents (mIPSCs) are thought to correspond to the responses elicited by the presynaptic release of a single vesicle of GABA[18]. Increases in the amplitudes of mEPSCs and mIPSCs reflects postsynaptic transmission strengthening, while increases in the event frequency reflect increases in the number of functional synapses or the presynaptic release probability[11].
   1. Fill the patch recording pipette with modified intracellular solution (Table 4) to adjust the reversal potential of the $GABA_A$ receptor-mediated current to -60 mV.
   2. Add 0.5 µM tetrodotoxin to the bath to block spontaneous action potentials.
   3. Hold the voltage at -60 mV to record the mEPSC events for 5 min.
   4. Change the holding potential to 0 mV to record mIPSC events for 5 min. Because M1 neurons show slightly higher reversal potential for AMPA receptor-mediated currents, the mIPSCs of M1 neurons are recorded at +15 mV with 0.1 mM APV.
   5. Wait for a few minutes for the current to stabilize.
   6. Record the mIPSC events for 5 min.
   7. Detect the miniature events using the software, and use events above 10 pA for the analysis. Count the number of mEPSCs or mIPSCs events for 5 min to determine the frequency. Average the amplitudes of the events to obtain the mean amplitude.
   8. Confirm whether bath treatment with 10 µM CNQX or with 10 µM bicuculline methiodide blocks the mEPSCs and mIPSCs events, respectively.

3. Paired-pulse analysis
   NOTE: Presynaptic plasticity can be analyzed using paired-pulse analysis. An increase in the paired-pulse rate suggests a decrease in the presynaptic glutamate or GABA release probability[7,10,11].
   1. To analyze excitatory synapses, add 0.1 mM picrotoxin and record the response at -60 mV. Although we added 4 µM 2-chloroadenosine to the bath, we need to keep in mind that the drug affects the presynaptic release probability[14].
   2. To analyze inhibitory synapses, add 0.1 mM APV and 4 µM 2-chloroadenosine to the bath and record the response at 0 mV. In M1 neurons, record the response at +15 mV.
   3. Apply paired pulses with an inter-stimulus interval of 100 ms or 200 ms.
   4. Record 50-100 sequential traces at each holding potential and average the values.
   5. Calculate the paired pulse ratio as the ratio of the second peak to the first peak of the postsynaptic current.

## Representative Results

As we described recently[7], rotor rod training (**Figure 1A**) induced dynamic changes in the intrinsic plasticity of the M1 layer II/III pyramidal neurons. Measuring the latency until the rats fall from the rotating rod allows us to estimate the skilled learning performance of the rat. Longer latency indicates better motor performance. On the day 1 of training, the rats improved their rotor rod performance until the trial ended. On day 2, the rats attained nearly asymptotic levels in the averaged session scores (**Figure 1B**). Compared with the latency at the first trial, *post-hoc* analysis showed significant improvements at the final trials on the training days (**Figure 1C**).

**Figure 4A** shows an example of current-clamp analysis in which the neuronal properties changed after motor skill learning. Injections of 400 pA and 500 pA currents were needed to induce action potentials in the untrained group and in the 1-day trained rats, respectively. In contrast, injection of only a 150 pA current was sufficient to elicit action potentials in the 2-day trained rats. The relationship between the current intensity and the number of action potentials is shown in **Figure 4B**. As little as 50 pA current was sufficient to elicit spikes in 2-day trained rats; in contrast, 1-day trained rats responded with fewer action potentials than untrained rats to 350 pA and higher currents. Moreover, **Figure 4C** shows that 1-day trained rats showed lower resting potential, higher spike threshold, and deeper afterhyperpolarization, whereas 2-day trained rats showed higher resting potential (**Figure 4C**) and membrane resistance (**Figure 4D**).

As we described previously[11], IA training (**Figure 1D**) induced postsynaptic plasticity at excitatory and inhibitory synapses of the hippocampal CA1 neurons. By measuring the latency in the light box, we could estimate the contextual learning performance of the rat. **Figure 1E** shows the results of the IA task. After the paired electric shock, the rats learn to avoid the dark side of the box and stay in the lighted side, which usually they would not prefer. The tendency to avoid the dark side therefore indicates the acquisition of contextual memories.

**Figure 5** shows an example of voltage-clamp analysis in which miniature postsynaptic currents were dramatically changed after contextual learning. To investigate learning-induced plasticity, spontaneous AMPA-mediated mEPSCs and $GABA_A$-mediated mIPSCs were sequentially recorded in the presence of 0.5 μM tetrodotoxin (**Figure 5A** and **B**). As shown on two-dimensional plots (**Figure 5C**), each CA1 neuron had different mean amplitudes for mEPSCs and mIPSCs. Although the amplitudes were low and showed a narrow distribution range in untrained, unpaired, and walk-through rats, those were diverse in IA-trained rats (Table 5). ANOVA followed by *post-hoc* analysis showed a significant increase in the mean amplitudes of mEPSC and mIPSC in IA-trained rats (**Figure 5E**), suggesting learning-induced postsynaptic plasticity in the CA1 neurons.

Moreover, each CA1 neuron exhibited different mEPSC and mIPSC frequencies (**Figure 5D**). Although the frequencies were low and showed a narrow distribution range in untrained, unpaired, and walk-through rats, those were diverse in IA-trained rats (Table 6). ANOVA followed by *post-hoc* analysis showed a significant increase in the frequencies of the mEPSC and mIPSC events in IA-trained rats (**Figure 5F**). There are two possible interpretations of these results. The first is that contextual learning increased the number of functional synapses of the neurons. The other is that contextual learning increased the presynaptic release probability of glutamate and GABA.

To further examine presynaptic plasticity, we also conducted paired-pulse stimulations, as reported previously[10,11].

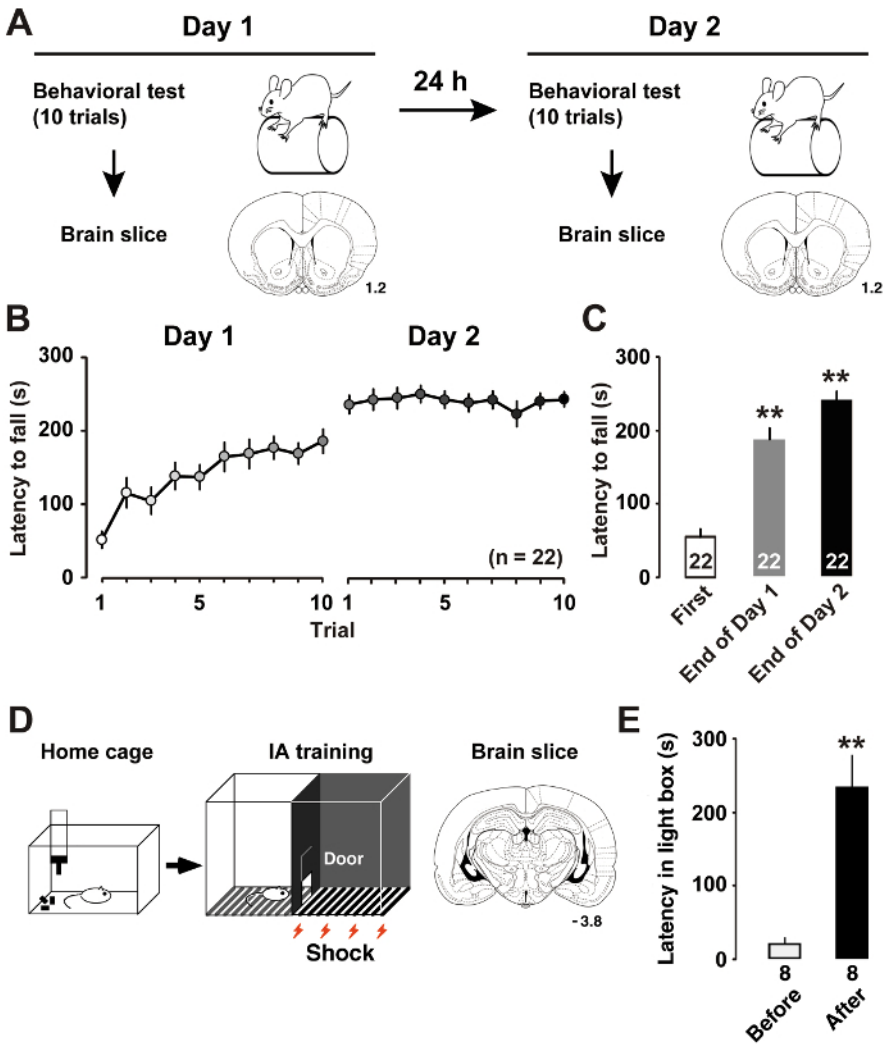


**Figure 1: Learning performance after training.**
*A*: The experimental design shows the rotor rod training and coronal brain slice. *B*: The mean latency to fall from the accelerating rotor rod barrel. *C*: The mean latency to fall off of the rod on the first and the final trials on training days 1 and 2[7]. ***P*<0.01 *vs.* first trial. *D*: Schema of the inhibitory avoidance (IA) task and coronal brain slice. *E*: The mean latency to enter the dark box before and after IA training[11]. ***P*<0.01 *vs.* before IA training. The numbers by the coronal sections indicate the distance anterior to the bregma in mm. The number of animals is shown at the bottom of the bars. Error bars indicate SEM. Please click here to view a larger version of this figure.

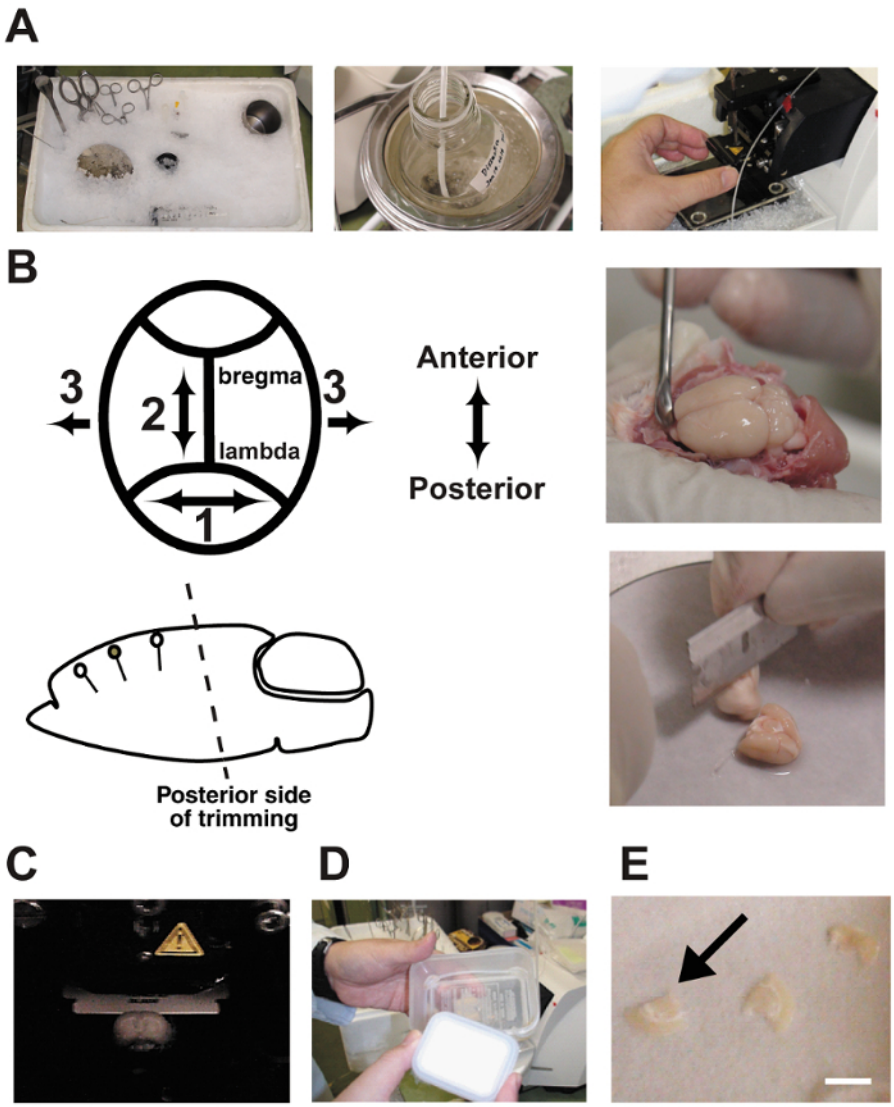


**Figure 2: Slice procedures.**
*A*: Photographs show the preparation of acute brain slices. The dissection tools were cooled in crushed ice prior to use. *B*: Brain dissection and trimming. Note that the angle of trimming on the posterior side must be oriented in parallel with the dendritic orientation. *C*: Slicing the brain in a vibratome chamber. The brain is bathed in dissection buffer and bubbled continuously with a 5% $CO_2$/95% $O_2$ gas mixture. *D*: An interface chamber made of two plastic food containers and a silicone tube. The chamber was filled with artificial CSF and bubbled continuously with the gas mixture. *E*: Brain slices were placed on wet filter paper in the chamber. Bar = 5 mm. Please click here to view a larger version of this figure.

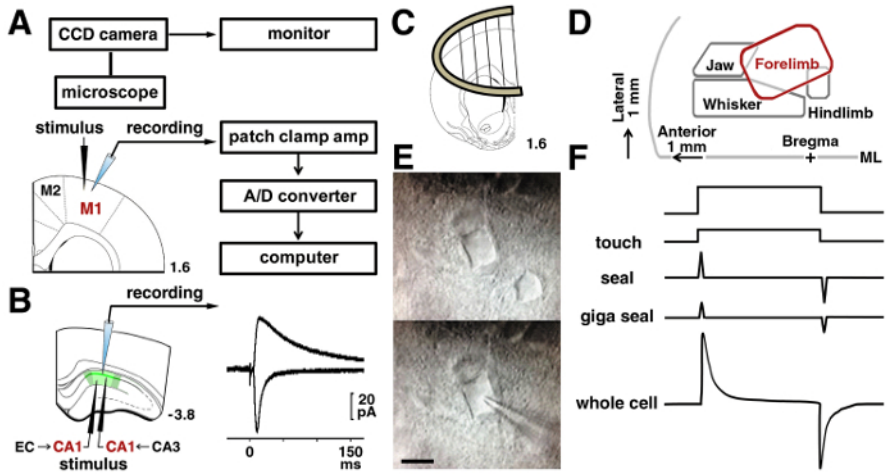


**Figure 3: Patch clamp procedures.**
*A*: The patch-clamp system used to record electrical signals from a neuron. The location of the stimulating and recording electrodes in the layer II/III neurons are shown in the rat motor cortex. *B*: To analyze the Schaffer synapses of a CA1 pyramidal neuron, a stimulating electrode was placed at the stratum radiatum. To analyze temporoammonic synapses, a stimulating electrode was placed at the stratum moleculare. Representative traces of evoked AMPA and NMDA receptor-mediated excitatory postsynaptic currents in the same CA1 neuron are shown. *C*: A slice anchor was used to stabilize the slice in the recording chamber. *D*: A representation map in the motor cortex, based on the published papers[15,16,17]. ML = midline. *E:* IR-DIC micrographs of M1 layer II/III neurons before *(upper*) and during the recording (*lower*). Bar = 10 µm. *F*: Changes in the pipette current before touch (*top*) and at membrane rupture (*bottom*). Please click here to view a larger version of this figure.

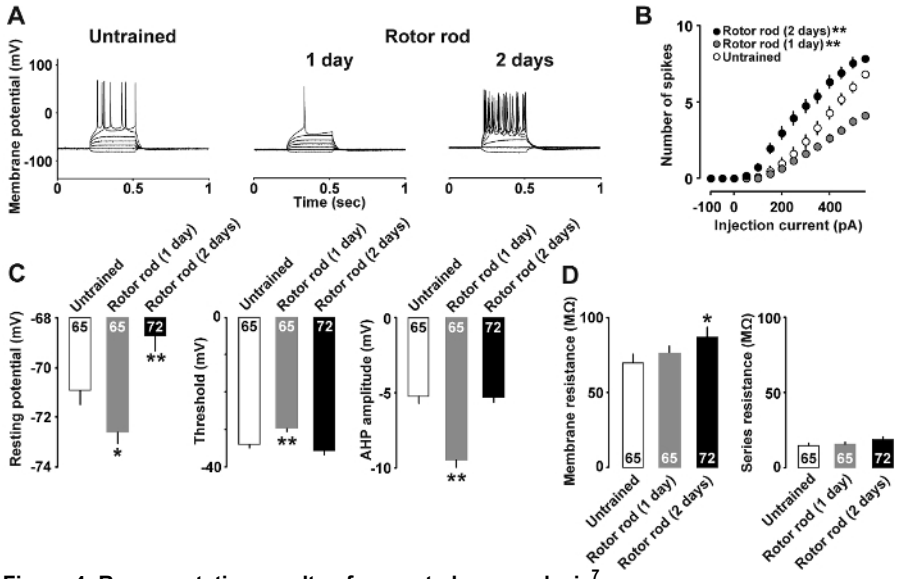


**Figure 4: Representative results of current-clamp analysis[7].**
*A*: Representative traces of action potentials recorded after induction with current injections. *B*: Relationships between the mean current input (pA) vs. action potential output (number of spikes) in brain slices from untrained (open bars), 1-day trained (gray bars), and 2-day trained rats (filled bars). *C*: Resting potential, threshold, and afterhyperpolarization of the layer II/III neurons. *D*: Membrane resistance and series resistance of the neurons. We used 9 - 10 rats in each group. The number of cells is shown within each bar. Error bars indicate the SEM. *$P$<0.05, **$P$<0.01 *vs.* untrained. Please click here to view a larger version of this figure.

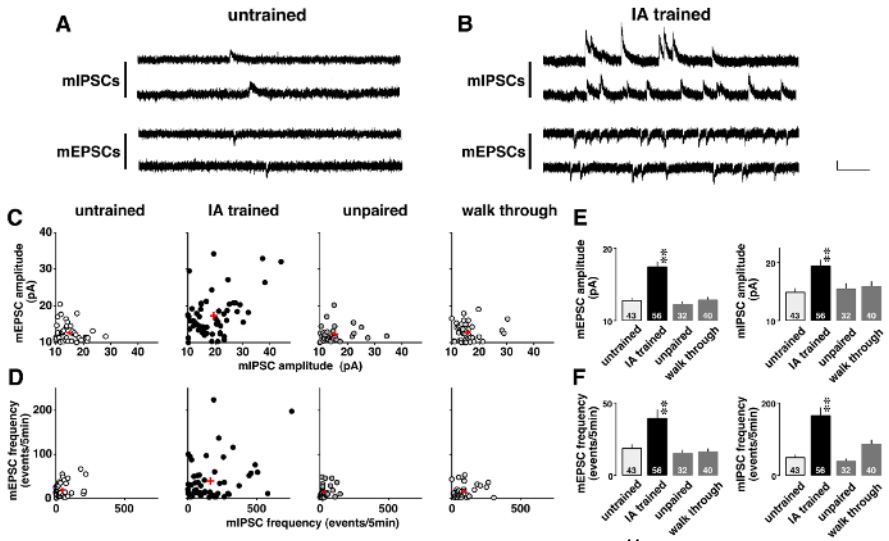


**Figure 5: Representative results of the voltage-clamp analysis[11].**
Representative traces of miniature excitatory and inhibitory postsynaptic currents (mEPSCs and mIPSCs) in untrained (*A*) and inhibitory avoidance (IA)-trained rats (*B*). mEPSCs at -60 mV and mIPSCs at 0 mV were measured sequentially in the same CA1 pyramidal neuron in the presence of tetrodotoxin (0.5 µM). Vertical bar = 20 pA, horizontal bar = 200 msec. *C*: Two-dimensional plots of the mean mE(I)PSC amplitudes in untrained, IA-trained, unpaired, and walk-through rats. *D*: Two-dimensional plots of the mE(I)PSC frequencies in the 4 groups. Note that each CA1 neuron exhibited different mean mE(I)PSC amplitudes and frequencies. IA training not only strengthened the mean amplitudes *(E)* but also increased the frequencies of the mE(I)PSC events *(F)*. We used 4 - 6 rats in each group. The number of cells is shown at the bottom of the bars. Red plus signs (*C, D*) and bars with vertical lines (*E, F*) indicate the mean ± SEM. ***P*<0.01 *vs.* untrained rats. Please click here to view a larger version of this figure.

| Dissection buffer (Total 1L) | | |
|---|---|---|
| $NaH_2PO_4 \cdot 2H_2O$ | 0.195 g | 1.25 mmol/L |
| KCl | 0.188 g | 2.5 mmol/L |
| $CaCl_2$ | 0.074 g | 0.5 mmol/L |
| $MgCl_2 \cdot 6H_2O$ | 1.423 g | 7.0 mmol/L |
| Choline chloride | 12.579 g | 90 mmol/L |
| Ascorbic acid | 2.340 g | 11.6 mmol/L |
| Pyruvic acid | 0.342 g | 3.1 mmol/L |
| $NaHCO_3$ | 2.100 g | 25 mmol/L |
| Glucose | 4.500 g | 25 mmol/L |

**Table 1: A recipe for dissection buffer**

| Artificial CSF (Total 1L) | | |
|---|---|---|
| KCl | 0.186 g | 2.5 mmol/L |
| NaCl | 6.700 g | 114.6 mmol/L |
| $NaH_2PO4 \cdot 2H_2O$ | 0.156 g | 1 mmol/L |
| Glucose | 1.800 g | 10 mmol/L |
| $NaHCO_3$ | 2.184 g | 26 mmol/L |
| 1M $MgCl_2$ | 4 mL | 4 mmol/L |
| 1M $CaCl_2$ | 4 mL | 4 mmol/L |

**Table 2: A recipe for artificial cerebrospinal fluid (CSF)**

| Intracellular solution for current clamp (Total 200 mL) | | |
|---|---|---|
| KCl | 0.0746 g | 5 mmol/L |
| K-Gluconate | 6.089 g | 130 mmol/L |
| HEPES | 0.476 g | 10 mmol/L |
| EGTA | 0.0456 g | 0.6 mmol/L |
| 1M $MgCl_2$ | 500 µL | 2.5 mmol/L |
| $Na_2$ ATP | 0.4408 g | 4 mmol/L |
| $Na_3$ GTP | 0.0418 g | 0.4 mmol/L |
| Na phosphocreatine | 0.510 g | 10 mmol/L |

**Table 3: A recipe for an intracellular solution for current clamp recording**

| Intracellular solution for voltage clamp (Total 200 mL) | | | | |
|---|---|---|---|---|
| $CsMeSO_3$ | 5.244 g | (5.814)* | 115 mmol/L | (127.5)* |
| CsCl | 0.672 g | (0.252)* | 20 mmol/L | (7.5)* |
| HEPES | 0.476 g | | 10 mmol/L | |
| EGTA | 0.0456 g | | 0.6 mmol/L | |
| 1M $MgCl_2$ | 500 µL | | 2.5 mmol/L | |
| $Na_2$ ATP | 0.4408 g | | 4 mmol/L | |
| $Na_3$ GTP | 0.0418 g | | 0.4 mmol/L | |
| Na phosphocreatine | 0.510 g | | 10 mmol/L | |
| * low $Cl^-$ concentration for miniature recordings | | | | |

**Table 4: A recipe for an intracellular solution for voltage clamp recording**

| Parameters | | untrained | IA trained | unpaired | walk through |
|---|---|---|---|---|---|
| mEPSC amplitude | Variance | 5.8 | 32.1 | 4.7 | 5.9 |
| | Standard deviation | 2.4 | 5.7 | 2.2 | 2.4 |
| | Coefficient of variation | 0.189 | 0.326 | 0.177 | 0.190 |
| mIPSC amplitude | Variance | 17.1 | 56.7 | 31.8 | 20.7 |
| | Standard deviation | 4.1 | 7.5 | 5.6 | 4.5 |
| | Coefficient of variation | 0.279 | 0.387 | 0.367 | 0.286 |

**Table 5: The diversity of miniature excitatory and inhibitory postsynaptic current (mEPSC and mIPSC) amplitudes in inhibitory avoidance (IA)-trained rats**

| Parameters | | untrained | IA trained | unpaired | walk through |
|---|---|---|---|---|---|
| mEPSC frequency | Variance | 278 | 2195 | 188 | 195 |
| | Standard deviation | 17 | 47 | 14 | 14 |
| | Coefficient of variation | 0.902 | 1.198 | 0.893 | 0.874 |
| mIPSC frequency | Variance | 3282 | 27212 | 1385 | 5135 |
| | Standard deviation | 57 | 165 | 37 | 72 |
| | Coefficient of variation | 1.195 | 1.006 | 0.955 | 0.836 |

**Table 6: The diversity of miniature excitatory and inhibitory postsynaptic current (mEPSC and mIPSC) frequencies in inhibitory avoidance (IA)-trained rats**

## Discussion

The major limitation of the slice patch clamp technique is the recording in slice preparation, which may not reflect what happens *in vivo*. Although *in vivo* current-clamp analysis is more reliable, it is technically challenging to get sufficient data from conscious animals. Since each pyramidal neuron has different cellular properties, an adequate number of cells is needed to properly analyze differences in neurons after training. Moreover, voltage-clamp analysis requires continuous drug treatment with CNQX, APV, or bicuculline to determine the nature of the postsynaptic

responses. To analyze the miniature responses induced by a single vesicle of glutamate or GABA, continuous treatment with tetrodotoxin is needed to block spontaneous action potentials. Although the recently developed multi-photon imaging technique is powerful for analyzing morphological changes at excitatory synapses[19], a combined patch clamp technique is needed to analyze the function of synapses *in vivo*. It is currently quite difficult to analyze morphological changes at inhibitory synapses, since most inhibitory synapses do not form spines. At this time, the slice patch clamp would be the most suitable technique to analyze cell properties or the functions of excitatory/inhibitory synapses in trained animals.

Using current-clamp analysis (**Figure 4**), we recently reported motor learning-induced intrinsic plasticity in layer II/III neurons. Specifically, the 1-day trained rats showed a significant decrease in resting membrane potential and an increase in the spike threshold. The 2-day trained rats showed a significant increase in resting membrane potential that led to increased excitability. These results suggested that there were dynamic changes in the intrinsic plasticity of M1 layer II/III neurons in trained rats. Additional voltage-clamp analysis revealed an increase in the paired-pulse ratio in 1-day trained rats, suggesting that there was a transient decrease in the presynaptic GABA release probability[7]. It is therefore possible that disinhibition from GABA at the layer II/III synapses might trigger the resulting learning-induced plasticity in the M1. In support of this, slice preparation of the M1 requires bath treatment with a $GABA_A$ receptor blocker to induce LTP[20].

Analysis of miniature postsynaptic potentials is a powerful way to detect synaptic plasticity in IA-trained animals. Sequential recording of mEPSCs and mIPSCs in a single CA1 neuron allows the analysis of the synaptic excitatory/inhibitory strength of each individual neuron. Since a single mE(I)PSC response is attributed to a single vesicle of glutamate or GABA, an increase in the mE(I)PSC amplitude suggests postsynaptic strengthening. Using mE(I)PSC analysis, we found individual differences in the strength of excitatory/inhibitory input into each CA1 neuron (**Figure 5C**). IA training clearly promoted diversity in synaptic strength, but this was not observed in other groups (Table 5).

Learning-induced synaptic diversity can be analyzed mathematically. By calculating the appearance probability of each point, data from each neuron can be converted to self-entropy (bit) using the information theory of Claude E. Shannon[21]. A point with high appearance probability (around the mean level) indicates low self-entropy, while a point with very rare probability (a deviated point) indicates high self-entropy. Compared with untrained rats, the self-entropy per neuron was clearly increased in IA-trained rats but not in unpaired or walk-through rats[22]. This analysis suggests that there was an increase in intra-CA1 information after the contextual learning.

The slice patch clamp technique can also be used for cued fear conditioning studies in the lateral amygdala[9] and for sensory experience studies in the barrel cortex[8]. Moreover, this technique can be used with various other techniques for further investigations. For instance, the virus-mediated green fluorescent protein (GFP)-tagged gene delivery technique can be combined with the patch clamp technique to analyze the function of specific molecules. In addition, focal microinjection of a retrograde tracer can be used to visualize specific neurons that project to a specific area. Then, using the current-clamp technique, cell-specific properties can be analyzed in the visualized neurons[23]. Further, combining two-photon laser-scanning microscopy with two-photon laser uncaging of glutamate has been used to demonstrate spine-specific growth and the EPSC response in mouse cortical layer II/III pyramidal neurons[19]. Thus, the slice patch clamp technique is being improved by combining it with novel chemicals, gene delivery, and photo manipulation techniques.

## Disclosures

The authors declare no conflicts of interest. We confirm that we have read the Journal's position on issues involved in ethical publication, and we affirm that this report is consistent with those guidelines. The funders had no role in the study design, data collection or analysis, the decision to publish, or the preparation of the manuscript.

## Acknowledgements

We would like to thank Dr. Paw-Min-Thein-Oo, Dr. Han-Thiri-Zin, and Mrs. H. Tsurutani for their technical assistance. This project was supported by Grants-in-Aid for Young Scientists (H.K. and Y.S.), Scientific Research B (D.M.), Scientific Research C (D.M.), and Scientific Research in Innovative Areas (D.M.), from the Ministry of Education, Culture, Sports, Science, and Technology of Japan.

## References

1. Neher, E., & Sakmann, B. Single-channel currents recorded from membrane of denervated frog muscle fibres. *Nature.* **260** (5554), 799-802 (1976).
2. Hamill, O. P., Marty, A., Neher, E., Sakmann, B., & Sigworth, F. J. Improved patch-clamp techniques for high-resolution current recording from cells and cell-free membrane patches. *Pflugers Arch.* **391** (2), 85-100 (1981).
3. Edwards, F. A., Konnerth, A., Sakmann, B., & Takahashi, T. A thin slice preparation for patch clamp recordings from neurones of the mammalian central nervous system. *Pflugers Arch.* **414** (5), 600-612 (1989).
4. Rioult-Pedotti, M. S., Friedman, D., & Donoghue, J. P. Learning-induced LTP in neocortex. *Science.* **290** (5491), 533-536 (2000).
5. Yang, G., Pan, F., & Gan, W. B. Stably maintained dendritic spines are associated with lifelong memories. *Nature.* **462** (7275), 920-924 (2009).
6. Xu, T. *et al.* Rapid formation and selective stabilization of synapses for enduring motor memories. *Nature.* **462** (7275), 915-919 (2009).
7. Kida, H. *et al.* Motor Training Promotes Both Synaptic and Intrinsic Plasticity of Layer II/III Pyramidal Neurons in the Primary Motor Cortex. *Cereb Cortex.* **26** (8), 3494-3507 (2016).
8. Takahashi, T., Svoboda, K., & Malinow, R. Experience strengthening transmission by driving AMPA receptors into synapses. *Science.* **299** (5612), 1585-1588 (2003).
9. Rumpel, S., LeDoux, J., Zador, A., & Malinow, R. Postsynaptic receptor trafficking underlying a form of associative learning. *Science.* **308** (5718), 83-88 (2005).
10. Mitsushima, D., Ishihara, K., Sano, A., Kessels, H. W., & Takahashi, T. Contextual learning requires synaptic AMPA receptor delivery in the hippocampus. *Proc Natl Acad Sci U S A.* **108** (30), 12503-12508 (2011).

11. Mitsushima, D., Sano, A., & Takahashi, T. A cholinergic trigger drives learning-induced plasticity at hippocampal synapses. *Nat Commun.* **4**, 2760 (2013).
12. Kida, H., & Mitsushima, D. Patch Clamp Technique in Brain Slices: Recording of Neuronal Activity in the Rat Primary Motor Cortex. *Yamaguchi Medical Journal.* **63** (2014).
13. Watt, A. J., van Rossum, M. C., MacLeod, K. M., Nelson, S. B., & Turrigiano, G. G. Activity coregulates quantal AMPA and NMDA currents at neocortical synapses. *Neuron.* **26** (3), 659-670 (2000).
14. Baidan, L. V., Zholos, A. V., & Wood, J. D. Modulation of calcium currents by G-proteins and adenosine receptors in myenteric neurones cultured from adult guinea-pig small intestine. *Br J Pharmacol.* **116** (2), 1882-1886 (1995).
15. Tandon, S., Kambi, N., & Jain, N. Overlapping representations of the neck and whiskers in the rat motor cortex revealed by mapping at different anaesthetic depths. *Eur J Neurosci.* **27** (1), 228-237 (2008).
16. Adachi, K., Murray, G. M., Lee, J. C., & Sessle, B. J. Noxious lingual stimulation influences the excitability of the face primary motor cerebral cortex (face MI) in the rat. *J Neurophysiol.* **100** (3), 1234-1244 (2008).
17. Tennant, K. A. *et al.* The organization of the forelimb representation of the C57BL/6 mouse motor cortex as defined by intracortical microstimulation and cytoarchitecture. *Cereb Cortex.* **21** (4), 865-876 (2011).
18. Pinheiro, P. S., & Mulle, C. Presynaptic glutamate receptors: physiological functions and mechanisms of action. *Nat Rev Neurosci.* **9** (6), 423-436 (2008).
19. Kwon, H. B., & Sabatini, B. L. Glutamate induces de novo growth of functional spines in developing cortex. *Nature.* **474** (7349), 100-104 (2011).
20. Hess, G., & Donoghue, J. P. Long-term potentiation of horizontal connections provides a mechanism to reorganize cortical motor maps. *J Neurophysiol.* **71** (6), 2543-2547 (1994).
21. Shannon, C. E. A mathematical theory of communication. . *Bell Sys Tech J.* **27** (1948).
22. Ono, K. M., D. Learning creates diversity of excitatory and inhibitory synapses in the hippocampal CA1: a possible amount of information at a single synapse. *J Physiol Sci.* **67 suppl 1** (2017).
23. Wang, L., Conner, J. M., Rickert, J., & Tuszynski, M. H. Structural plasticity within highly specific neuronal populations identifies a unique parcellation of motor learning in the adult brain. *Proc Natl Acad Sci U S A.* **108** (6), 2545-2550 (2011).